

Time resolution optimization for the future LHCb Electromagnetic Calorimeter

A. BELLAVISTA(*)

INFN, Sezione di Bologna - Bologna, Italy

Dipartimento di Fisica e Astronomia Augusto Righi, Università di Bologna - Bologna, Italy

Summary. — Starting from Run 5 of the LHC, LHCb will operate at luminosities up to $1.5 \times 10^{34} \text{ cm}^{-2}\text{s}^{-1}$, requiring major upgrades to its Electromagnetic Calorimeter. The new detector must withstand high radiation doses and achieve time resolutions of a few tens of picoseconds to suppress pile-up effects. The inner and high-occupancy regions of the upgraded calorimeter — named PicoCal — will adopt a Spaghetti Calorimeter (SpaCal) design, using scintillating fibres embedded in a dense absorber and read out by photomultiplier tubes (PMTs). The choice of PMT is crucial to achieve the required timing performance. Simulations of single-sided readout modules (with PMTs only on the downstream side) show that fast PMTs can yield worse time resolutions due to longitudinal fluctuations of the electromagnetic showers, which bias the signal timestamps. A correlation between signal rise time and shower depth was also observed. To address this, a rise-time-based correction method was developed, significantly improving the timing resolution. Testbeam measurements with electron energies up to 100 GeV confirmed the approach, achieving resolutions below 20 ps and demonstrating good timing capabilities even with single-sided readout.

1. — Introduction

In order to maximize the physics opportunities presented by the high-luminosity phase of the LHC [1], the LHCb experiment will undergo a second major upgrade—referred to as LHCb Upgrade II—during the LHC’s fourth Long Shutdown period (LS4). Beginning with Run 5, LHCb will operate at a peak luminosity of $1.5 \times 10^{34} \text{ cm}^{-2}\text{s}^{-1}$. To cope with the elevated particle rate, a substantial enhancement of the Electromagnetic Calorimeter (ECAL) is essential, as it will be subjected to radiation doses reaching up to 1 MGy in its innermost region. The upgraded calorimeter, named PicoCal, must also provide timing information with a resolution of few tens of picoseconds to mitigate pile-up effects [2].

(*) on behalf of the LHCb ECAL Upgrade II R&D group

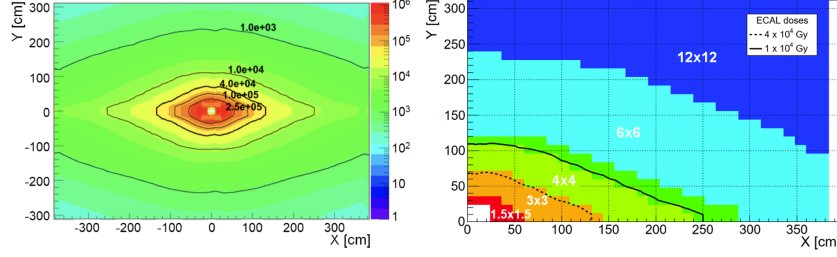


Fig. 1. – (Left) Expected absorbed radiation dose (in Gray) for the LHCb PicoCal modules at the end of their operational lifetime, as a function of their position on the PicoCal surface [5]. (Right) Cell dimensions (in cm) across the various regions of the PicoCal [2].

Furthermore, its energy resolution must remain similar to the current one, *i.e.* $\sigma(E)/E \sim 10\%/\sqrt{E} \oplus 1\%$.

The present LHCb ECAL consists of Shashlik modules composed of alternating layers of 4 mm thick plastic scintillator tiles and 2 mm thick lead sheets [4]. The new detection concept being developed is based on a Spaghetti Calorimeter (SpaCal) architecture, which features scintillating fibres—made of polystyrene or garnet crystal—embedded within a dense passive absorber (lead or tungsten). Light generated by particle interactions with the fibres will be read out using photomultiplier tubes (PMTs).

Following LS4, the proposed baseline design for PicoCal comprises SpaCal-W modules that incorporate tungsten absorbers and radiation hard inorganic crystal fibres in the innermost zone. The intermediate region will utilize lead absorbers combined with plastic polystyrene fibres (SpaCal-Pb), while the outermost region will employ Shashlik modules with varying levels of granularity. Each calorimeter module will be divided longitudinally into upstream (front) and downstream (back) sections, separated by a mirror and equipped with PMTs on both ends to enable double-sided readout. The arrangement of these modules will follow a rhomboidal geometry, tailored to correspond with the distribution of occupancy and radiation dose across the PicoCal surface [2], as depicted in fig. 1.

During the LS3 phase, the detector will undergo improvements involving the replacement of the innermost Shashlik modules with SpaCal-W and SpaCal-Pb modules that utilize polystyrene scintillating fibres [3]. These new modules will feature a single-sided readout design, incorporating PMTs on the downstream end only, while the front part will be equipped with a mirror to enhance light collection efficiency. This approach offers a cost-effective alternative to the double-sided readout configuration. As a result, there is ongoing evaluation of the potential to extend the use of these single-readout modules into Run 5, provided they satisfy the required performance criteria. A schematic comparison of the two module types is shown in fig. 2. Due to the reduced cost, this solution would also allow to increase the detector granularity in the single-sided regions. The following sections present studies on the time resolution of single-sided readout modules.

2. – Simulations of a Pb-Polystyrene module

Simulations of a lead-polystyrene module in a single-sided readout configuration were performed to investigate the time resolution as a function of the PMT response speed,

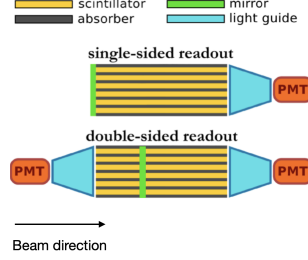


Fig. 2. – Schematic illustration comparing SpaCal modules with single-sided (top) and double-sided (bottom) readout configurations.

using incident electrons with energies of 1 GeV and 10 GeV.

The timestamp of pulses generated by incident electrons was extracted using the Constant Fraction Discriminator (CFD) method, which determines the time at which the signal crosses a fixed fraction of its maximum amplitude. The CFD threshold was optimized to yield the best overall time resolution, defined as the standard deviation of the timestamps distribution.

As expected, 10 GeV electrons result in improved time resolution compared to 1 GeV electrons. However, slower PMTs demonstrated better timing performance than their faster counterparts. This counterintuitive behavior arises from the longitudinal fluctuations of the electromagnetic showers along the detector depth. In particular, the CFD timestamp is correlated with the shower depth—defined as the average energy-weighted longitudinal position of the energy depositions within the fibres. Two opposing effects are observed; in fact, for deeper showers:

- direct photons (emitted towards the readout PMTs) tend to arrive earlier, introducing a negative correlation;
- reflected photons arrive later on average, creating a positive correlation.

These correlations are more pronounced with faster PMTs, which are more sensitive to differences in photon arrival times, leading to variations in signal shape. Since the CFD algorithm does not account for these shape distortions, the resulting timestamps exhibit increased spread, thus degrading time resolution. Moreover, the extent of these effects depends on the selected CFD threshold: lower thresholds are more influenced by direct photons, while higher thresholds are dominated by reflected ones. At intermediate values, the opposing correlations can partially cancel, reducing the overall bias.

To mitigate this bias, a preliminary correction method has been developed. The approach involves constructing a calibration curve f by means of a polynomial fit to the CFD timestamp as a function of shower depth. For each event j , the corrected timestamp is defined as $\hat{t}_j \doteq t_j - f_j$, where t_j is the original timestamp and f_j is the fitted correction curve evaluated at the event's shower depth. Following this correction, the optimal CFD threshold may shift compared to the uncorrected case. The corrected time resolution is then defined as the standard deviation of the corrected timestamp distribution.

3. – Testbeam results

A testbeam campaign was carried out at the CERN SPS in June 2024 to study the performance of various SpaCal and Shashlik modules using electron and hadron beams with energies ranging from 20 GeV to 100 GeV. This section focuses on the time resolution measurements of a SpaCal-W module constructed with polystyrene scintillating fibres and exposed to electron beams impinging the centre of one cell of the prototype. The tested module consists of four cells, each with a transverse area of $2 \times 2 \text{ cm}^2$.

The study includes a comparison between two fibre types—Kuraray SCSF-78 and 3HF, which emit blue and green light, respectively—and four candidate PMT models: Hamamatsu R14755U-100, R9880U-20, R7600U-20, and R11187⁽¹⁾.

Figure 3 presents the measured time resolution as a function of the incident electron energy for all four PMTs. SCSF-78 fibres consistently yield better time resolution compared to the 3HF ones, primarily due to their faster scintillation decay time. Among the tested PMTs, the slower-response models (R7600U-20 and R11187) show the best performance when paired with SCSF-78 fibres, in agreement with prior simulation results. In contrast, for the 3HF fibres, the optimal time resolution is achieved using PMTs with Extended Red Multi-Alkali (ERMA) photocathodes—specifically R7600U-20 and R9880U-20—which offer improved quantum efficiency in the green spectral range.

Simulations indicate a strong correlation between the shower depth and the rise time of the readout signals. This relationship enables the application of the correction procedure outlined in the previous section by using the signal rise time as a proxy for the shower depth, since the latter is not directly measurable. The time resolution obtained with the fastest PMTs (R14755U-100 and R9880U-20) shows more significant improvements following this correction. As illustrated in fig. 4, time resolutions better than 20 ps were achieved at high energies, with the best performance observed for the combination of SCSF-78 fibres and the R7600U-20 PMT.

In addition, testbeam measurements have been performed at DESY (Hamburg), employing incident electrons between 1 GeV and 5 GeV. Different fibres have been tested: Kuraray SCSF-78, Kuraray 3HF, Kuraray 3HF bundled together (i.e. grouped together by a bundler when they come out of the back section) and fibres produced by Luxium. The results before and after the above-described correction procedure are shown in fig. 5. In this lower energy regime, the bias correction is effective only for the Kuraray SCSF-78 fibres, which feature the fastest scintillation kinetics.

4. – Conclusions

Simulation studies and testbeam analyses have been carried out on SpaCal modules operating in single-sided readout mode. The focus was on evaluating the time resolution with incident electrons and understanding how longitudinal fluctuations of electromagnetic showers affect the measurements.

⁽¹⁾ PMTs were optically coupled to the fibres using 5 cm long light guides. A delayed-wire-chamber detector was employed to select events where electrons impinged on a $10 \times 10 \text{ mm}^2$ area around the cell's centre. The timing reference was provided by two microchannel-plate (MCP) detectors, offering a combined time resolution of approximately 15 ps. Signal digitization was performed using a DRS4-based CAEN V1742 digitizer operating at 5 GS/s. The time-resolution results reported here are corrected for contributions from both the reference time and electronic noise.

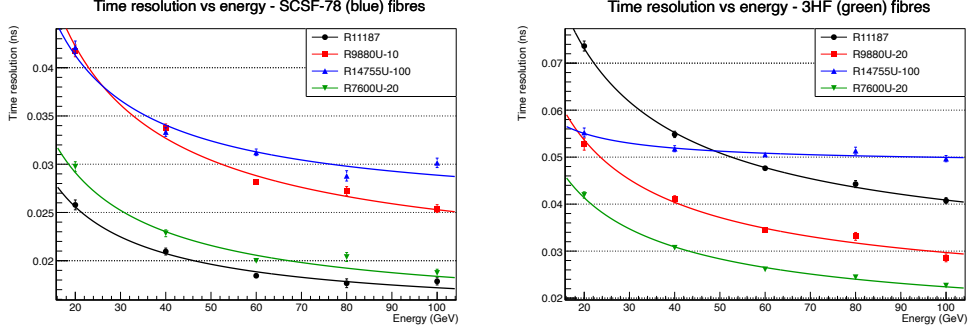


Fig. 3. – Measured time resolution as a function of incident electron energy before applying the correction procedure. The data are fitted using a function defined as the quadrature sum of a stochastic term and a constant term: $\sigma_t(E) = s/\sqrt{E} \oplus c$. Results are shown for the four tested PMTs using SCSF-78 fibres (left) and 3HF fibres (right).

Simulations revealed that the CFD timestamp is biased by the electromagnetic showers depth, degrading the time resolution. To mitigate this, a correction procedure was developed. The effect is more pronounced for fast PMTs, whose sharper response makes the signal shape more sensitive to shower fluctuations—an effect not accounted for by the CFD algorithm [6].

Testbeam data collected in 2024 were used to compare different PMT models and types of polystyrene fibres. The correction was applied using the signals rise time as a proxy for showers depth. This approach proved effective and promising for the PicoCal R&D. Time resolutions below 20 ps were achieved at electron energies above 50 GeV, confirming the good timing capabilities of the SpaCal modules even with single-sided readout.

* * *

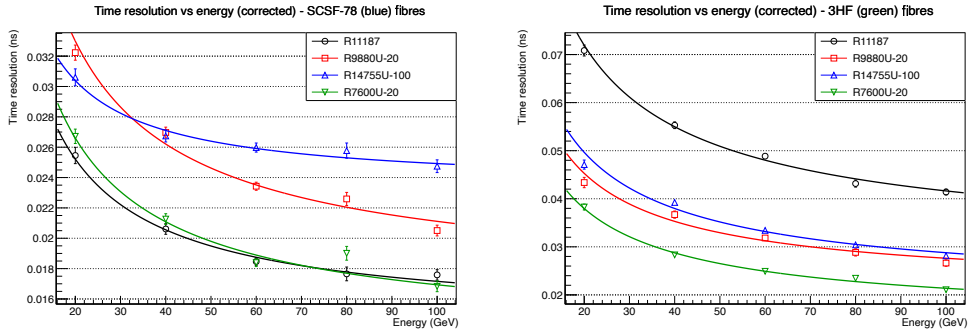


Fig. 4. – Measured time resolution as a function of incident electron energy after applying the correction procedure. The data are fitted using a function defined as the quadrature sum of a stochastic term and a constant term: $\sigma_t(E) = s/\sqrt{E} \oplus c$. Results are shown for the four tested PMTs using SCSF-78 fibres (left) and 3HF fibres (right).

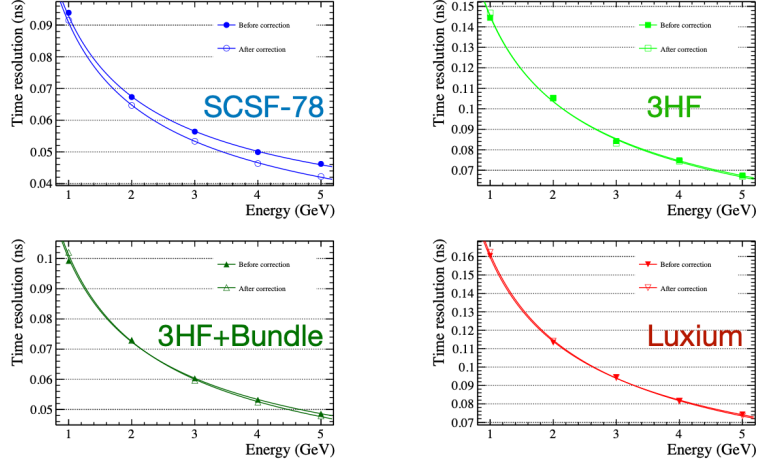


Fig. 5. – Measured time resolution at DESY (Hamburg) as a function of incident electron energy before and after applying the correction procedure, for four different kinds of fibres.

This work was supported by Italian Ministero dell'Università e Ricerca (MUR) and European Union - Next Generation EU through the research grant number PRIN-2022MHC2MH, CUP I53D23001310006, under the program PRIN 2022.

REFERENCES

- [1] LHCb COLLABORATION, CERN Report LHCb-PUB-2018-009, CERN-LHCC-2018-027, LHCC-G-171, Geneva (2016), [arXiv:1808.08865](https://arxiv.org/abs/1808.08865).
- [2] LHCb COLLABORATION, CERN Report CERN-LHCC-2023-005, LHCb-TDR-024, Geneva (2023) .
- [3] KHOLODENKO S., *Nucl. Instrum. Methods Phys. Res., A*, **1066** (2024) 169656 .
- [4] LHCb COLLABORATION, *JINST*, **3** (2008) S08005, https://cds.cern.ch/record/1129809/files/jinst8_08_s08005.pdf.
- [5] LHCb COLLABORATION, CERN Report CERN-LHCC-2021-012, LHCb-TDR-023, Geneva (2021), <https://cds.cern.ch/record/2776420>.
- [6] BELLAVISTA A., CERN-THESIS-2024-322, Master's thesis, IMAPP Master Degree (2024).